UNIVERSITY OF OKLAHOMA

GRADUATE COLLEGE

EVOLUTION OF THE HYDROTHERMAL STAGE WITHIN MIAROLITIC CAVITIES IN GRANITIC PEGMATITES OF CALIFORNIA AND MAINE, USA

A THESIS

SUBMITTED TO THE GRADUATE FACULTY

in partial fulfillment of the requirements for the

Degree of

MASTER OF SCIENCE

By

CHARLES LORIN DUVAL

Norman, Oklahoma 2019

EVOLUTION OF THE HYDROTHERMAL STAGE WITHIN MIAROLITIC CAVITIES IN GRANITIC PEGMATITES OF CALIFORNIA AND MAINE, USA

A THESIS APPROVED FOR THE

SCHOOL OF GEOSCIENCES

BY

Dr. David London, Chair

Dr. Andrew S. Elwood Madden

Dr. Megan E. Elwood Madden

Table of Contents

Abstract

Clay and alkali feldspar samples from miarolitic cavities of the pegmatites of Maine and California provide some of the best lines of evidence for gaining a better understanding of the hydrothermal stage within the pockets. X-ray diffraction (XRD) and energy dispersive x-ray analysis (EDXA) were used to analyze the mineralogy and chemistry of clay samples, and x-ray diffraction was used to determine the Al/Si order of the alkali feldspars. Clay samples are composed primarily of montmorillonite and kaolinite and in a few cases, illite, laumontite, and cookeite. A variety of other minerals is present within, including traces of primary pocket-forming minerals of quartz, albite, and microcline, in addition to oxides of goethite and todorokite. According to x-ray diffraction patterns from the International Centre for Diffraction Data (ICDD), three different patterns ($Na_{0.3}(Al,Mg)_2Si_4O_{10}(OH)_2 \cdot xH_2O$; $(Ca,Na)_{0.3}Al_2(Si,Al)_4O_{10}(OH)_2 \cdot xH_2O$; $Ca_{0.2}(Al,Mg)_2Si_4O_{10}(OH)_2 \cdot 4H_2O$) best fit the montmorillonite minerals in the samples. The main distinction within these mineral varieties is the elements that occupy the interlayer and octahedral sites within the mineral. Energy dispersive x-ray analysis of the eight samples that are dominantly montmorillonite, showed some variation in magnesium and calcium values, 0.71-2.58 weight percent for magnesium and 1.48-2.14 weight percent for calcium. All samples showed essentially no presence of sodium. There were no clear correlations between the values from EDXA analyses and the varieties identified in the XRD patterns.

Alkali feldspar samples from miarolitic cavities yielded Al/Si order values in the range of 0.85 to 1.02, which were found to be indicative of recrystallization of the primary-formed feldspars. Alkali feldspars with high Al/Si order values indicate evidence of extensive recrystallization of the primary-formed feldspars within the miarolitic cavities and has been linked to a higher activity of H_2O in the pegmatitic melt. With the presence of primary-formed

minerals, zeolites, and clay minerals, evidence supports hydrothermal alteration of the aluminosilicate glass from the fluid exsolved from the pegmatitic melt and of later-stage hydrothermal alteration involving the host rock and primary minerals. The fluid begins as an alkaline-rich one and transitions to an acid-rich phase, precipitating zeolite minerals followed by smectite and finally kaolinite.

1. INTRODUCTION/PROBLEM STATEMENT

London (2008) defines pegmatite as "an essentially igneous rock, commonly of granitic composition, that is distinguished from other igneous rocks by its extremely coarse but variable grain-size, or by an abundance of crystals with skeletal, graphic, or other strongly directional growth-habits". As summarized by London (2008), the formation of pegmatitic rocks has been debated extensively for many years, beginning with De Beaumont (1847) and Hitchcock (1883) who suggested an igneous origin for pegmatites and Hunt (1871) who suggested a hydrothermal origin. Lindgren (1913, 1937) then proposed a continuum in which pegmatites began forming as igneous rocks and then later transitioned to a more hydrothermal environment. Later, Jahns and Burnham (1969) proposed the idea that pegmatites form due to exsolution of an aqueous vapor phase from the melt. The presence of this phase paired with incongruent partitioning of potassium over sodium into the aqueous phase resulted in the unique textures and zonation of minerals within pegmatites. This concept, for many years, has been the most widely recognized model. London (2008) has since suggested the idea that most aspects of pegmatite formation are largely due to liquidus undercooling of a granitic melt.

Over the years, one of the main topics of discussion has centered around the presence and importance of an aqueous fluid phase as being necessary to produce pegmatites. Although the pegmatitic rocks themselves are igneous in origin, the only definitive evidence of an aqueous phase is the presence of miarolitic cavities, or crystal-filled pockets, some of which can contain gem-grade minerals (London 2008, 2013). When present in pegmatites, miarolitic cavities generally occur near the centers of dikes, as represented by the areas outlined in blue in **Figure 1**. However, the formation of these pockets has remained unstudied. With so many gem and clay minerals found within these miarolitic cavities, gaining a better understanding of how these

pockets form and evolve could prove useful to miners and scientists in locating future deposits. The mines in southern California and in Maine are some of the only accessible pegmatites with miarolitic cavities, and therefore, analyzing samples from these localities provides a better understanding of the mineralogy and internal evolution of these pockets.

2. OBJECTIVES

This study focuses on the mineralogy of the clays from miarolitic cavities in pegmatites of the Oceanview and Himalaya mines in California and the pegmatites associated with the Havey, Mount Mica, and Plumbago Mountain mines in Maine. Additionally, the degree of Al/Si order of the alkali feldspars, including four from California and one from Maine, were assessed to better understand the hydrothermal stage in miarolitic cavities within pegmatites. In studying the clay and zeolite minerals from the pockets, the goal is to classify the minerals and determine their origin and the evolution of miarolitic cavities. In studying the Al/Si order of the alkali feldspars, the goal is to determine the degree of recrystallization of the initial pocket feldspar crystals to support or refute the presence of an aqueous phase during the formation of miarolitic cavities.

3. BACKGROUND

3.1 Minerals present within miarolitic cavities

There are a relatively small number of pegmatites that contain miarolitic cavities, and in the ones that do contain miarolitic cavities, the cavities only constitute less than 5% of the volume within a pegmatite (London 2013). Miarolitic cavities are open or clay-filled pockets within granitic pegmatites that can contain several unique and exotic minerals in addition to the common rock-forming minerals, quartz, albite, and alkali feldspar, as illustrated in **Figure 2** and **Figure 3**. These figures show two separate miarolitic cavities the first of which shows crystals

capped by a white and red clay and the second which shows gem elbaite within a rusty clay matrix. **Table 1** illustrates most of these minerals that can be present within pegmatites, including micas, beryl, elbaite, pollucite, montebrasite, spodumene, topaz, and the zeolite minerals, which form during the initial stages of the formation of the pockets from a flux-rich granitic melt. Other minerals, including the kaolin, smectite, chlorite, oxide, carbonate, and other phyllosilicate group minerals form at a later stage, potentially either just after the initial minerals form or long after they crystallize, because of hydrothermal alteration of the primary-formed materials and leaching of components from the host rock.

It is known that liquidus undercooling of about 200°C of the melt plays a significant role in the formation of pegmatitic pockets, and that because of this undercooling, the pocket minerals crystallize at temperatures around 350-400°C (London 1986, Morgan and London 1999, London et al., London 2008, London 2012). The model proposed by London (2009,2013) best describes the formation of the first-formed crystals within miarolitic cavities and the clay matrix that is characteristic of pockets as well. In this model, the fluid begins as a low viscosity aluminosilicate melt that contains a boundary layer liquid enriched in flux components, including boron, lithium, phosphorus, fluorine, and an aqueous phase. As these elements are collected within this boundary layer, their concentrations increase enough to crystallize tourmaline, montebrasite, topaz, and other exotic minerals, which eventually depletes the melt of the flux components. As the gem crystals form, the water finally exsolves leaving behind clear, pristine crystals. As the remainder of the aluminosilicate liquid cools, the viscosity increases and suspends the crystals in a glass, which is later altered to the clay matrix that is characteristic of many miarolitic cavities.

Three zeolite minerals, heulandite, laumontite, and stilbite, have also been observed in miarolitic cavities at numerous localities by various authors (Roger 1910, Jahns and Wright 1951, Foord et al. 1986). These minerals have a relatively low thermal stability and are formed at temperatures below the formation of the main crystals that crystallize out of the melt. In studies on the thermal stabilities of these three minerals, at 200 MPa, the pressure that corresponds to the depth at which miarolitic pegmatites form (London 1986), the zeolite stilbite decomposes to heulandite around 170°C, in the presence of excess quartz and H_2O (Liou 1971a). At this same pressure, heulandite decomposes to laumontite around 180°C (Cho, et al. 1987), and laumontite decomposes to wairakite, $Ca(Al_2Si_4O_{12}) \cdot 2H_2O$, around 282°C (Liou 1971b). Although the zeolite minerals most often form as products of hydrothermal alteration of volcanic glass in a variety of environments, feldspars and smectite group minerals can be zeolite parent materials as well, and the mineralogy is strongly determined by the temperature of the environment (Marantos et al. 2012). Laumontite commonly dehydrates and is found in powder form in pockets (Coombs 1952), but stilbite and heulandite are found on the primary-formed crystals, which are all hosted in the clay matrix.

The last minerals to form within the pocket sequence are the clay minerals that suspend the primary-formed crystals. Two minerals that compose this matrix are kaolinite and montmorillonite, which are known to be stable at temperatures up to 300°C but can be formed at temperatures well below that (Vidal et al. 2012). Montmorillonite and other smectite group minerals can be formed as secondary replacement minerals due to hydrothermal alteration and leaching of constituents from the surrounding host rock. For example, many pegmatites in southern California intruded into the San Marcos Gabbro (Fischer 2011). This type of host rock, which is composed of pyroxenes and plagioclase with lesser amounts of olivine and amphibole,

can contain the cations, primarily iron, magnesium, and calcium, needed to create these secondary minerals. However, if these elements are originally present within the pegmatitic melt, they would likely partition into a mineral like tourmaline, for example, at the onset of crystallization of the miarolitic cavity. Because these cations are incompatible in the melt relative to the mineral, they are not present within the melt during the later stages of formation and would therefore need to come from another source.

Kaolinite, which likely forms from alteration of the last quenched glass from the aluminosilicate melt, can also form from hydrothermal alteration of primary pocket feldspars. Kaolinite is a pure white clay, but in the samples from the Himalaya mine noted by Foord et al. (1986) and the samples from the Himalaya and Oceanview mines in this study, kaolinite-rich clays are iron-stained and red-orange in color. For this reason and its presence within veins and fractures, Foord et al. (1986) suggested a late-stage supergene occurrence for this mineral. Cookeite, a lithium-bearing chlorite group mineral, is another alteration mineral of primary-formed spodumene crystals and has been called a "snow-on-the-roof" mineral because of its occurrence on the tops of tourmaline, quartz, feldspars, and other primary pocket minerals. These secondary minerals and others similar in composition can all form in lower temperature environments in comparison with the primary pocket crystals.

3.2 Prior studies

Some of the earliest analyses of clay minerals associated with pegmatites were conducted by Schaller (1925) and Laudermilk and Woodford (1934), in which they noted the presence of halloysite and montmorillonite, respectively, in association with a granitic pegmatite. These authors attributed their occurrences to weathering as opposed to hydrothermal alteration. Oyawoye and Hirst (1964) also noted the presence of a montmorillonite with a granite in Nigeria

but concluded that the clay was of primary origin because it occurred in the presence of unaltered, fresh rock. Jahns and Wright (1951) observed clays in California pegmatites and suggested two different types of origin, one of hypogene in which the clays formed at the same time as the rest of the crystals and the other of supergene in which the clays precipitated because of the breakdown of minerals in the presence of some aqueous phase. Aside from these few studies, the clay minerals and their origin were of little importance to the miners in the early days who were primarily looking for the gem minerals.

However, the presence of clays plays an important role in further understanding the conditions of formation within the pockets (London 2013). In many miarolitic cavities, single crystals of quartz, topaz, tourmaline, and other minerals are hosted within the clay minerals or at the bottom of dry pockets. This indicates most, if not all, of the clay minerals formed during the very end stages of pocket formation, and in the case of the dry pockets, the clay slowly weathered away, allowing the crystals to settle at the bottom of the pockets (London 2013). London (2009, 2013) proposed the idea that the minerals that compose the clay matrix within a miarolitic cavity form from alteration of a last-formed glass. Initially, the primary minerals, including tourmaline, topaz, quartz and feldspars, crystallize from a flux-rich aluminosilicate melt. As the melt cools, the final liquid forms a glass, and this glass later alters to the clay matrix via interaction from hydrothermal fluids. In their Table 8, London and Morgan (2017) have shown that this glass contains the elements needed, primarily silicon, aluminum, and various alkali metals to form the clay minerals. However, it could be possible that other cations could enter the pocket from the host rock at a later stage.

Stilbite, heulandite, and laumontite, all form at lower temperatures minerals than the primary-formed crystals. They must have formed at some point between the formations of the

primary crystals and the clay minerals because they are found on the surfaces of these crystals suspended in clay. London and Burt (1982) propose a model of evolution of miarolitic cavities based on alteration of primary-formed lithium aluminosilicates. They suggest that after the primary crystals form, the minerals undergo subsolidus metasomatism in which the pegmatitic fluid exchanges sodium and calcium for lithium resulting in deposition of albite and calcium-rich phosphate minerals, which is then followed by a fluid enriched in phosphorus and fluorine volatiles that deposits secondary mica. This evolution of the fluid represents chemical change from a fluid that is more alkaline to one that is more acidic in composition. Because stilbite, heulandite, and laumontite are all hydrated calcium aluminosilicates that form at or below temperatures around 280°C, they could likely crystallize from this alkaline-rich exsolved fluid. This stage is then followed by the formation of the minerals that are representative of the clay matrix.

Prior to this study, there has been only one principal study in which clays from different pegmatites were analyzed and identified in detail, mostly from the Himalaya Mine with fewer samples from surrounding mines, including the Katrina, White Queen, Oceanview, and Little Three mines, in southern California (Foord et al. 1986). After observing the pockets in the field, they utilized bulk and clay fraction x-ray diffraction mounts, petrographic microscopes, and x-ray fluorescence, to determine the mineralogy and chemistry of the minerals. They noted the presence of stilbite, laumontite, cookeite, Li-tosudite, beidellite, Mg-Ca montmorillonite, palygorskite, and calcite. Also, they confirmed the idea presented by Jahns and Wright (1951) that there were two types of clays, one white-pink, hypogene smectite deposited in an alkaline environment and one red-brown, supergene kaolinite deposited in an acid environment. The authors propose a model of pocket formation which starts with the tourmaline, quartz, feldspars,

and other such minerals. The pocket then ruptures, and the clay and zeolite minerals form afterward, beginning with smectite, primarily Ca-Mg montmorillonite, followed by the zeolite minerals stilbite and laumontite, and finally kaolinite at the very end stage. Because there's no presence of calcium and magnesium are not present in the primary-formed crystals. Therefore, those components must have come from the norite host rock. This indicates that smectite forms due to hydrothermal alteration of the host rock. Foord et al. (1986) suggest kaolinite forms near the very end of the clay formation, as the smectite minerals undergo further alteration near the surface. Their interpretations of the origin of the clay minerals within the pegmatites therefore rely solely on the chemistry of the environment and depth at the time of deposition.

This method of clay formation by Foord et al. (1986) presents a contradiction with what London (2009, 2013) has proposed. In the Foord model, the components to create smectite, specifically Ca-Mg montmorillonite are leached from the surrounding host rock during pegmatite formation to create the clay, and then further alteration of the pocket minerals at the very end of the formation of the miarolitic cavity creates kaolinite. On the other hand, London suggests that the clay matrix is resultant from hydrothermal alteration of the last-formed glass a cooled aluminosilicate liquid. Kaolin and smectite group minerals can likely both form from alteration of the glass. London agrees that there likely is some interaction with the host rock due to ferric iron present in red-orange kaolinite, but most of the constituents necessary to form the clay are present in the pocket.

In their paper, Foord et al. (1986) also discuss the presence of quartz, spodumene, feldspars, and mica in the Himalaya and Little Three dikes as commonly being etched or corroded within the matrix of montmorillonite or kaolinite. The quartz, spodumene, feldspars assemblage suggest formation from an aluminosilicate rich melt. Looking at the clay minerals

that generally make up the matrix in which these primary crystals are suspended, the kaolin and smectite group ones, the constituents to form these minerals are already present within the melt and the primary-formed minerals. Therefore, it is possible that some of the clay minerals could have formed from the breakdown of the primary-formed minerals, in addition to interaction with the country rock.

Within miarolitic cavities, primary alkali feldspars can be (1) completely unaltered, (2) etched, indicating they have undergone dissolution and are left with a porous texture or have undergone alteration and new minerals have been formed on their surface, or (3) recrystallized, meaning the primary-formed crystals can have a perthitic texture and a glassy overgrowth on the first formed crystals. Because kaolinite has been known to form as an alteration product of feldspar, there is a possibility that some of the clay minerals formed due to the alteration or breakdown of the primary-formed alkali feldspar, so studying these feldspar crystals would prove beneficial in understanding the processes that occur within miarolitic cavities. London et al. (2012) analyzed the degree of Al/Si order within feldspar samples from the Swamp dike at the Little Three Mine in Ramona, California, utilizing the methodology of Kroll and Ribbe (1987). Kroll and Ribbe (1987) originally used cell parameters in monoclinic and triclinic alkali feldspars to form equations that showed the distribution of aluminum and silicon among the four tetrahedral sites in the feldspar. From these equations, they determined that a higher Al/Si order value was indicative of recrystallization of the crystal. Using this study as a guideline, London et al. (2012) analyzed feldspars from different zones in the Swamp dike, Little Three mine, Ramona, California, and noticed the Al/Si order gradually increases towards the center of the dike, meaning the original, disordered crystals lie towards the margins of the dike, whereas the feldspars near the center, where the pockets would be, are more ordered and show evidence of

recrystallization. Parsons and Lee (2009) found a correlation between the activity of H_2O and the Al/Si order of the feldspars, suggesting that the more ordered crystals were associated with the higher activity of H_2O and, thus, recrystallization of the primary crystals.

4. CLAY SAMPLE LOCAATIONS

4.1 California

The Oceanview Mine is owned by Jeff Swanger and is located within the San Jacinto Mountains in northwestern San Diego County in the Pala District near Pala, California. The Pala District is home to some of the most famous pegmatite mines in California, including the Stewart, Tourmaline King, Tourmaline Queen, and Pala Chief mines. These mines have produced numerous pockets of gem-grade minerals, including tourmaline, beryl, and spodumene. Purple gem-grade spodumene, termed kunzite, from this area is some of the finest in the world. The Oceanview Mine is no different than these other mines and is a source of gem-grade aquamarine, morganite, and the best kunzite in North America. The Himalaya Mine is owned by Chris Rose and is located just to the southeast of the Pala District in the Mesa Grande District in north central San Diego County near Mesa Grande, California. Like the Oceanview mine, the Himalaya mine has produced many gem minerals, most notably pink and green gem-grade tourmaline. Unlike at the Oceanview mine, though, kunzite is not found in the abundance in the Mesa Grande District compared to the Pala District (Fisher 2011).

The pegmatites associated with this area intrude and are hosted within rocks from the Peninsular Ranges Batholith, which is Cretaceous in age (Larsen 1948). There are several plutons that comprise this batholith, and the host rock for many of the pegmatites is the San Marcos Gabbro, estimated to be between 135 and 105 Ma, and the pegmatitic dikes have been estimated to have an emplacement age of around 98-89 Ma (Kampf, Gochenour, and Clanin

2003). The pegmatites, compositionally, fall into the category of LCT, meaning they are enriched in lithium, cesium, and tantalum, according to Cerny's (1991) classification scheme. With the abundance of spodumene and lepidolite, it is evident that the melt from which these rocks crystallized was highly concentrated with lithium, and with tourmaline present as well, the melt was enriched in boron.

4.2 Maine

The Havey Mine owned by Jeff Morrison, located near Poland, Maine, and Mt. Mica and Plumbago Mountain, owned by Gary Freeman, located near Paris, Maine, all lie in the Oxford pegmatite field and are hosted in the rocks of the Central Maine Belt (Wise & Brown 2010). The rocks that make up this suite are Paleozoic sedimentary rocks intruded by Devonian to Permian igneous rocks (Solar & Brown 2001a, 2001b, Solar & Tomascak 2009, Tomascak et al. 1996). The Sebago pluton, where most of the pegmatites are found in the district, has been dated through uranium isotopes to be around 296-293 Ma (Foord et al. 1995, Tomascak et al. 1996). The pegmatites are classified as LCT and contain gem-grade tourmaline, montebrasite, pollucite, rose quartz, and various other rare earth element minerals.

5. ALKALI FELDSPAR SAMPLE LOCATIONS

The feldspars come primarily from the mines in southern California, including the White Queen, Oceanview, Himalaya, and Little Three mines, with the exception that one comes from Plumbago Mountain in Maine. All the feldspar samples are from the margins of the miarolitic cavities within their respective pegmatite dikes.

6. METHODOLOGY

The six clay samples from Maine were obtained through the mail directly from the miners, and the ten samples from California were either obtained from the miners in the field or

collected in the field. Seven of the alkali feldspar samples analyzed in this study were from the collection of Dr. David London, and one was collected in the field at the Himalaya Mine in California.

6.1 X-ray diffraction analysis of clay minerals

For analyses of the pocket clay samples, powder x-ray diffraction was the primary technique used, which utilized the Rigaku Ultima IV X-ray diffractometer at the University of Oklahoma and Cu-Kα radiation with a voltage of 40 kV and a current of 44 mA. Bulk random and oriented clay fraction mounts were made for each sample. The bulk random mounts were prepared by crushing the sample with a mortar and pestle, micronizing, and drying. Produced powders were analyzed using the Bragg-Brentano method with a count time of 2 seconds, step size of 0.02, rotating at 30 rpm, and over the duration of 2-70 2θ degrees. The clay fraction mounts were prepared by running the sample through a 2 mm sieve, dismembrating for 5 minutes, centrifuging at 800 rpm for 3.5 minutes, and utilizing the filter peel method, according to Drever (1973), to create the mount. Each clay fraction mount was analyzed three times, once as an air-dried sample, once after being saturated with ethylene glycol overnight, and once after being heated at 550°C for 1 hour, and using the Bragg-Brentano method with a count time of 2 seconds, step size of 0.02, no sample rotation, over the duration of 2-30 2θ degrees. Data analysis and phase identification were performed using MDI Jade 2010 with the ICDD PDF-4+ database. In addition to clay minerals, the zeolite minerals present within these samples were characterized because they crystallize under low metamorphic or hydrothermal conditions, like the clay minerals.

6.2 Electron microprobe analysis of clay minerals

To determine the chemistry of the clay samples that are primary composed of montmorillonite, these eight clay samples, two from Maine and six from California, were analyzed using a CAMECA SX100 electron probe micro-analyzer equipped with five wavelength-dispersive spectrometers at the University of Oklahoma by the electron microprobe operator Lindsey Hunt. All samples were analyzed at 15 kV accelerating voltage and a 1 μm spot size. All elements, Na, Mg, Al, Si, K, Ca, Ti, Mn, Fe, Rb, Cs, and Ba, were monitored using a sample current of 10 nA over the range of 60.0 seconds. The main objective in analyzing these clay samples was to observe what elements are present as the interlayer cations and within the octahedral sites.

6.3 X-ray diffraction analysis of alkali feldspars

The alkali feldspar samples were analyzed using the random mount method used for the clay samples. The conditions were changed to account for a closer look at the (060) and (204) peaks needed to calculate the Al/Si order of the sample. The Bragg-Brentano method was used with a count time of 4 seconds, step size of 0.01, rotating at 30 rpm, and over the duration of 40-52 2θ degrees. Data were analyzed using MDI Jade 2010 to determine the positions of the (060) and (204) peaks. Using equations 7 and 8 from Kroll and Ribbe (1987), which correspond to monoclinic and triclinic symmetries of alkali feldspars, the 2θ angle values for those peaks were used to calculate a value of the Al/Si ordering of each sample.

7. RESULTS

7.1 XRD of pocket clay samples

Data were collected from bulk and clay mounts of each clay sample. Based on diffraction patterns, mineral names were assigned to each peak within every spectrum. **Table 2** compiles the major (M), minor (m), and trace (tr) minerals present within each sample. Major

minerals in the context of this study are defined as the minerals that contain multiple peaks of diffraction with the greatest intensities, minor minerals as the ones that contain a few peaks with weaker intensities, and trace minerals as ones that contain only the major diffraction peak characteristic of the mineral with a very weak intensity. Of the sixteen samples, eight contained mostly montmorillonite, five mostly kaolinite, and one of each of muscovite, cookeite, and laumontite. Because there is less variation between the chemical compositions within kaolinite, illite, laumontite, and cookeite, the samples dominated by those minerals do not need to be analyzed further. However, the montmorillonite can show variation in elements that are present within the interlayer and octahedral sites, so further analyses are beneficial to better constrain their chemical signatures.

Of the samples containing primarily montmorillonite, there were best fits with patterns from the International Centre for Diffraction Data (ICDD) database for three compositionally different reference patterns of montmorillonite shown in **Table 3**. Of the three different chemical signatures, two can contain magnesium in the octahedral site, one contains just sodium as the interlayer cation, one contains just calcium as the interlayer cation, and one can contain a combination of sodium and calcium as the interlayer cations. Of the eight samples, seven of them are dominated by one primary montmorillonite variety, while one, OVU 007, contains roughly equal amounts of two montmorillonite varieties.

7.2 EDXA of pocket clay samples

To confirm the compositions of the smectite clays within samples MM 1, MM 3, OVU 002, OVU 003, OVU 004, OVU 007, HIM 026, and HIM 028, each sample was analyzed using EDXA. X-ray diffraction data revealed all these clay samples to contain mostly montmorillonite. In comparing the number of cations of the elements within each sample, each

one showed values representative of montmorillonite varieties in the ICDD database. The elemental values obtained are shown in **Table 4**. These analyses were also conducted to determine if there were any unique elemental signatures within them the samples, such as elevated weight percentages of iron or sodium, indicative of other smectite group minerals, but all samples had roughly the same abundance of constituents, representative of montmorillonite. From XRD analyses, the main difference in varieties is with the presence of sodium, calcium, and magnesium. In each sample, sodium values are 0.02 weight percent or below, insignificant values compared to calcium and magnesium. Three of the samples can contain magnesium in the octahedral sites, OVU 003, OVU 007, and HIM 026, data from EDXA shows weight percent values of 0.80%, 2.58%, and 1.49% for each sample, respectively. The other samples in which magnesium was not present in the chemical formula, according to XRD patterns, had magnesium values that ranged from 0.71 weight % to 2.49 weight %. Calcium weight percentages are in the range of 1.48-2.24%. Elevated weight percentages of manganese, weight percent values of 3.42% and 4.42%, and of iron, 4.63% and 3.05%, are present within samples OVU 002 and OVU 003. The manganese and iron are not likely present within the structures of the clays, but rather as oxide minerals, such as goethite and todorokite found during XRD analyses. Overall, very few correlations could be made in comparing the elemental signatures from EDXA data and the patterns from XRD data, as evidenced by **Figures 4, 5,** and **6**, which show scatter plots of the relationships between Ca and Mg, Si and Al, and Mg and Al, respectively. As these values fluctuate within a sample, it would be expected that they change accordingly. For example, if there is more Mg in a sample, it would be expected to see potentially lower Al and Ca values as those elements occupy the sites in which Mg is present within the samples. Upon comparing these elements, no clear correlations could be made.

7.3 Al-Si order of alkali feldspar samples

Upon analysis of the potassium feldspar crystals, the Σt_1 values calculated using equations 7 and 8 from Kroll and Ribbe (1987) are shown in **Table 5**, and correspond to monoclinic and triclinic feldspars, respectively. Because the crystal system is not known for the feldspar samples, both equations are used to compute Al/Si order values, but there is minimal difference in each sample. However, based on the computed values, specific terms defined by Kroll and Ribbe (1987) could be assigned to each sample. According to their study, values between 0.80 and 0.90 are termed "adularia", which is an intermediate between disordered orthoclase and ordered microcline. Values between 0.90 and 1.0 are termed microcline. Parsons and Lee (2009) attributed the high Al/Si order to recrystallization of the primary, disordered alkali feldspars to secondary, ordered alkali feldspars. An increase in Al/Si order has been interpreted to correlate with an increase in the activity of H_2O in the melt (London et al. 2012). In theory then, there would be ordered microcline near the centers of the pegmatite dikes and less ordered orthoclase at the edges of the dikes.

8. DISCUSSION

To determine how and where the pocket clay minerals formed, it is necessary to know the extent of alteration to which the pocket minerals have been subjected and what processes caused the formation of those minerals. In order to form secondary minerals, including the zeolite and clay group minerals, it is evident that lower temperatures and alteration of primary-formed crystals and country rock are key during the evolution of the pocket. If the original matrix that suspends the primary crystals begins as an aluminosilicate glass, as suggested by London (2009, 2013), at some point after the primary crystals form, the contents within the miarolitic cavity are subjected to hydrothermal alteration to alter the glass to clay. With the presence of the zeolite

minerals perched on primary-formed quartz, feldspar, and other crystals, it is clear that the zeolites formed at some stage between the primary minerals and the clay matrix. Building on this idea, it seems quite evident that there are three stages during the formation of miarolitic cavities: the crystallization of the crystals from the pegmatitic melt, the formation of the lower temperature minerals, including the zeolites from the exsolved fluid, and even later crystallization of the clay minerals from alteration of the glass and leaching of constituents from the host rock. Pictured in **Figure** 7, Meunier (2005) has described the minerals that form in the presence of different hydrothermal systems with increasing hydrogen relative to alkalis when transitioning from alkaline to acidic environments. In an alkaline environment with the presence of calcium, the zeolites stilbite, heulandite, and laumontite form. In an intermediate environment with the presence of calcium and magnesium, smectite and chlorite minerals form. In an acidic environment lacking alkalis, kaolinite and cookeite form.

In their study, Foord et al. (1986) observed two primary clays, a lighter colored montmorillonite and a darker colored kaolinite. Based on their observations, they noted the kaolinite was iron-stained and the last formed mineral in the miarolitic cavities based on textural observations and finding it within fractures and cracks of the pockets. Based on these observations, it only seems logical that the authors would say the montmorillonite formed before the kaolinite. If the exsolved fluid from the melt transitions from alkaline to acidic in chemistry and montmorillonite forms in an alkaline-rich environment and kaolinite in an acid-rich environment, montmorillonite should crystallize prior to kaolinite. Kaolinite most commonly crystallizes as a result of the alteration of feldspars in granite. With this thought in mind and if the alkali feldspar crystals are etched, the kaolinite observed in these pockets could have formed from the alteration of these pocket feldspars. The fact that the clay is a darker red colored clay

with iron staining supports the idea that it likely precipitated much later and included iron oxide minerals from outside sources after the pocket was fully formed.

In the clay samples from California, the main mineral is kaolinite in three of them, montmorillonite in six of them, and laumontite in one of them. In the three kaolinite samples, the color of the clay is red-orange, likely due to some iron oxide staining. In the six montmorillonite samples, the color of the clay is pale to dark pink. These observations coincide almost identically with what Foord et al. (1986) observed. Because the clay samples in this study were collected by the miners, there is no way to know what other pocket minerals were present upon excavation of the clays. Therefore, it is not possible to either refute nor support Foord's claims. Based on these observations alone, though, it would make the most logical sense that the kaolinite found within these miarolitic cavities is formed at a much later stage in comparison with the rest of the pocket minerals.

The sample from California that is composed almost entirely of laumontite, HIM 027, is a white, granular sample. Laumontite is known to break down from its crystalline form into a powder when exposed to air (Coombs 1952). Unlike all the other samples, this one contained very few, if any, traces of a phyllosilicate group mineral. If it is assumed that the zeolite minerals form within pockets from the alkaline-rich fluid, this specific miarolitic cavity likely did not undergo the same processes than the pockets from all the other samples, meaning there is no evidence of an acid-rich fluid phase within this cavity. According to Meunier (2005), if only zeolite minerals are present, there is only evidence for the alkaline-rich stage of the fluid. It seems possible that the miarolitic cavity from which HIM 027 was collected was not subjected to the later occurrences of acidic hydrothermal alteration after the zeolite minerals.

Of the samples from Maine, the main mineral is kaolinite in two of them, montmorillonite in two of them, illite in one of them, and cookeite in one of them. Unlike the kaolinite samples from California, the samples from Maine are white in color. This observation shows that there are no other phases present when the clay was formed, unlike the iron oxide minerals in the kaolinite from the miarolitic cavities of California. Looking back at the model of pocket formation from London (2009, 2013), if there is little to no presence of alkalis within the last-formed glass, the glass would alter to a pure kaolinite. With the two samples from the Havey mine, since kaolinite is the major mineral present, it seems clear that the fluid that altered the last-formed glass was acidic in chemistry. As far as the two montmorillonite samples from Maine, magnesium and calcium elemental weight percentages obtained from EDXA are similar to weight percentages from the samples of California, which likely were introduced into the pocket via leaching from the host rock. In these miarolitic cavities, there seems to be only the presence of an alkaline-rich fluid and not an acid-rich one.

In looking at the alkali feldspar samples, five of them had Al/Si order values between 0.90 and 1.00, which according to Kroll and Ribbe (1987), are indicative of ordered microcline. The other three samples had values between 0.80 and 0.90, which is representative of an intermediate between disordered orthoclase and ordered microcline. Of the two rim and core pair samples, the LT3 044 and PbN Mbr samples, the rim, or glassy overgrowth, of the LT3 044 sample shows slightly more order while the core, or base, of the PbN Mbr sample shows slightly more order. Building on the idea that the higher Al/Si order values are a result of recrystallization of the pocket primary-formed alkali feldspars, samples HIM 024, OVU 008, and LT3 048 should be found closer to the edges of their respective pegmatites, and WQU 3, both LT3 044, and both PbN Mbr samples would have been found closer to the centers of their

respective pegmatites. Overall, with high Al/Si order values of the alkali feldspars, the presence of an aqueous phase within the miarolitic cavities is further supported.

9. CONCLUSIONS AND FUTURE WORK

Until recently, the clay and other secondary pocket minerals within miarolitic cavities have been largely overlooked. Scientists have observed them in the field and characterized them, but there have not been many studies that have taken an in-depth look at these minerals, specifically their nature of formation and their role within the formation of the miarolitic cavity. By analyzing the mineralogy and chemical signatures of the clays that suspend gem crystals of tourmaline, quartz, beryl, and spodumene within miarolitic cavities, the origin of their formation can be better understood. Montmorillonite and kaolinite, which are low temperature minerals, are the dominating clay minerals within these pockets. From previous studies, it is proposed that the constituents that are contained within the interlayer and octahedral sites within montmorillonite, calcium, magnesium, and iron, are leached into the pocket through contact with the country rock. Kaolinite is thought to be formed from hydrothermal alteration of the last bits of the aluminosilicate melt that forms the primary crystals, but there is also some debate that kaolinite comes in at even later stage because of its textural locations in fractures of the miarolitic cavities and iron staining within some miarolitic cavities in the pegmatites of California.

It seems clear that many pockets undergo some degree of alteration after they fully form. From past authors, this alteration can occur via the last fluid exsolved from the pegmatitic melt or later stage hydrothermal alteration from outside sources, causing constituents to be leached into the pockets from the host rock. As the fluid last present from the pegmatitic melt decreases in temperature, the chemistry evolves from one that is more alkaline to more acidic over time

(London and Burt 1982). As this fluid interacts with primary aluminosilicates, it alters their mineralogy. This study proposes a paragenetic sequence of the low-temperature minerals in which the zeolite minerals form first followed by smectite group minerals, including montmorillonite, followed by kaolinite. This model reflects the views of Meunier (2005), which shows a transition in chemistry of the fluid from one that is alkaline-rich to one that is acid-rich. The smectite, kaolin, and oxide group minerals can also form through hydrothermal alteration in contact with the host rock, which brings in the necessary components to crystallize these minerals. As another line of evidence, Al/Si order of alkali feldspar samples from miarolitic cavities show high values indicative of recrystallized orthoclase to microcline via H_2O interaction.

Because these clay sample locations and alkali feldspar locations did not coincide all that well, future studies could be conducted by observing spatial relations of the pocket minerals and collecting and analyzing samples from the same pocket. In observing the textures and location of the minerals within a pocket, the sequence of mineralization becomes more apparent. Observing the presence of the clay minerals, their locations of occurrence inside the miarolitic cavity, and their presence or lack thereof within fractures leading away from the pocket can all be lines of evidence in determining the evolution of the mineralization of the pocket. The presence of the zeolite minerals within many miarolitic cavities and the processes that govern their crystallization also poses a topic of interest that is still not well understood or studied. It is also apparent that XRD is useful in determining minerals present within a sample, but if chemical distinctions in varieties of minerals are preferred, EDXA proves to be more accurate than XRD. Additionally, solution chemistry, x-ray fluorescence, and transmission electron microscopy could also prove useful in better determining chemical compositions of the clay

minerals. Thermal stability and alkalinity/acidity experiments could also prove beneficial in observing what processes are at play during the crystallization of the minerals that form in the presence of the aqueous fluid during miarolitic cavity formation.

REFERENCES

Černý, P. (1991). Rare-element granitic pegmatites. Part I: anatomy and internal evolution of pegmatitic deposits. *Geoscience Canada*, *18*(2).

Cho, M., Maruyama, S., & Liou, J. G. (1987). An experimental investigation of heulandite-laumontite equilibrium at 1000 to 2000 bar P fluid. *Contributions to Mineralogy and Petrology*, *97*(1), 43-50.

Coombs, D. S. (1952). Cell size, optical properties and chemical composition of laumontite and leonhardite: With a Note on Regional Occurrences in New Zealand. *American Mineralogist: Journal of Earth and Planetary Materials*, *37*(9-10), 812-830.

De Beaumont, L. E. (1847). Note sur les émanations volcaniques et métallifères. *Société Géologique de France sér*. 4, 12, 1249.

Drever, J. I. (1973). The preparation of oriented clay mineral specimens for X-ray diffraction analysis by a filter-membrane peel technique. *American Mineralogist*, *58*, 553-554.

Eberl, D., & Hower, J. O. H. N. (1975). Kaolinite synthesis: The role of the Si/A1 and (alkali)/(H+) ratio in hydrothermal systems. *Clays and Clay Minerals*, *23*, 301-309.

Fisher, J. (2011). Mines and minerals of the Southern California pegmatite province. *Rocks & Minerals*, *86*(1), 14-35.

Foord, E.E., Snee, L.W., Aleinikoff, J.N., & King, V.T. (1995) Thermal histories of granitic pegmatites, western Maine, USA. Geological Society of America, Abstract, A-468.

Foord, E. E., Starkey, H. C., & Taggart, J. E. (1986). Mineralogy and paragenesis of" pocket" clays and associated minerals in complex granitic pegmatites, San Diego County, California. *American Mineralogist*, *71*(3-4), 428-439.

Hitchcock, E. (1883). Report on the geology, mineralogy, botany, and zoology of Massachusetts. *Massachusetts Geologic Survey Report*.

Hunt, T. S. (1871). Notes on granitic rocks. *American Journal of Science*, (3), 182-191.

Jahns, R. H., & Burnham, C. W. (1969). Experimental studies of pegmatite genesis; l, A model for the derivation and crystallization of granitic pegmatites. *Economic Geology*, *64*(8), 843-864.

Jahns, R. H., & Wright, L. A. (1951). *Gem-and lithium-bearing pegmatites of the Pala district, San Diego County, California*. State of California, Department of Natural Resources, Division of Mines.

Kampf, A. R., K. Gochenour, and J. Clanin. 2003. Tourmaline discovery at the Cryo-Genie mine, San Diego County, California. Rocks & Minerals 78 (3): 157–68.

Kroll, H., & Ribbe, P. H. (1987). Determining (Al, Si) distribution and strain in alkali feldspars using lattice parameters and diffraction-peak positions; a review. *American Mineralogist*, *72*(5-6), 491-506.

Larsen, E. S., Jr. 1948. Batholith and associated rocks of Corona, Elsinore, and San Luis Rey quadrangles, Southen California. Geological Society of America memoir 29.

Laudermilk, J. D., & Woodford, A. O. (1934). Secondary montmorillonite in a California pegmatite. *American Mineralogist: Journal of Earth and Planetary Materials*, *19*(6), 260-267.

Lindgren, W. (1913). *Mineral deposits*. McGraw-Hill, New York, N.Y.

Lindgren, W. (1937). Succession of minerals and temperatures of formation in ore deposits of magmatic affiliations. *Trans. Am. Inst. Mining & Metall. Eng*, *126*, 356-376.

Liou, J. (1971a). Stilbite-laumontite equilibrium. *Contributions to Mineralogy and Petrology*, *31*(3), 171-177.

Liou, J. G. (1971b). P—T Stabilities of Laumontite, Wairakite, Lawsonite, and Related Minerals

in the System CaAl2Si2O8-SiO2-H2O. *Journal of Petrology*, *12*(2), 379-411.

London, D. (1986). Formation of tourmaline-rich gem pockets in miarolitic pegmatites. *American Mineralogist*, *71*(3-4), 396-405.

London, D. (2008). *Pegmatites*. Quebec, Canada: Mineralogical Association of Canada.

London, D. (2009) The origin of primary textures in granitic pegmatites. Canadian Mineralogist, 47, 697-724.

London, D. (2013). Crystal-filled cavities in granitic pegmatites: Bursting the bubble. *Rocks & Minerals*, *88*(6), 527-538.

London, D., & Burt, D. M. (1982). Alteration of spodumene, montebrasite and lithiophilite in pegmatites of the White Picacho District, Arizona. *American Mineralogist*, *67*(1-2), 97-113.

London, D., & Morgan, G. B. (2017). Experimental crystallization of the Macusani obsidian, with applications to lithium-rich granitic pegmatites. *Journal of Petrology*, *58*(5), 1005-1030.

London, D., Morgan, G. B., Paul, K. A., & Guttery, B. M. (2012). Internal evolution of miarolitic granitic pegmatites at the Little Three mine, Ramona, California, USA. *The Canadian Mineralogist*, *50*(4), 1025-1054.

Oyawoye, M. O., & Hirst, D. M. (1964). Occurrence of a montmorillonite mineral in the Nigerian younger granites at Ropp, Plateau Province, northern Nigeria. *Clay Minerals*, *5*(32), 427-433.

Marantos, I., Christidis, G. E., & Ulmanu, M. (2012). Zeolite formation and deposits. *Handbook of natural zeolites*, 28-51.

Meunier, A. (2005). Hydrothermal Process—Thermal Metamorphism. *Clays*, 379-415.

Morgan, G. B., VI & London, D. (1999). Crystallization of the Little Three layered pegmatite-aplite dike, Ramona District, California. *Contributions to Mineralogy and Petrology, 136*(4), 310-330.

Parsons, I. & Lee, M.R. (2009): Mutual replacement reactions in alkali feldspars. I. Microtextures and mechanisms. *Contrib. Mineral. Petrol*. 157, 641-661.

Rogers, A. F. (1910). Minerals from the pegmatite veins of Rincon. *San Diego County, California: Columbia University School of Mines Quarterly, 31*, 208-218.

Schaller, W. T. (1925). The genesis of lithium pegmatites. *American Journal of Science*, (57), 269-279.

Solar, G.S. & Brown, M. (2001a) Deformation partitioning during transpression in response to Early Devonian oblique convergence, northern Appalachian orogeny, USA. *Journal of Structural Geology* 23, 1043–1065.

Solar, G.S. & Brown, M. (2001b) Petrogenesis of migmatites in Maine, USA: Possible source of peraluminous leucogranite in plutons? *Journal of Petrology* 42(4), 789–823.

Solar, G.S. & Tomascak, P.B. (2009) The Sebago pluton and the Sebago Migmatite Domain, Southern Maine: results from new studies. 2009 Annual Meeting of Northeastern Section, Geological Society of America, Field Trip 2, 1–24.

Tomascak, P.B., Krogstad, E.J., & Walker, R.J. (1996) U-Pb monazite geochronology of granitic rocks from Maine: implications for late Paleozoic tectonics in the Northern Appalachians. *The Journal of Geology* 104, 185–195.

Vidal, O., Baldeyrou, A., Beaufort, D., Fritz, B., Geoffroy, N., & Lanson, B. (2012). Experimental study of the stability and phase relations of clays at high temperature in a thermal gradient. *Clays and Clay Minerals, 60*(2), 200-255.

Wise, M.A. & Brown, C.D. (2010) Mineral chemistry, petrology and geochemistry of the Sebago granite-pegmatite system, southern Maine, USA. *Journal of Geosciences* 55, 3–26.

FIGURES

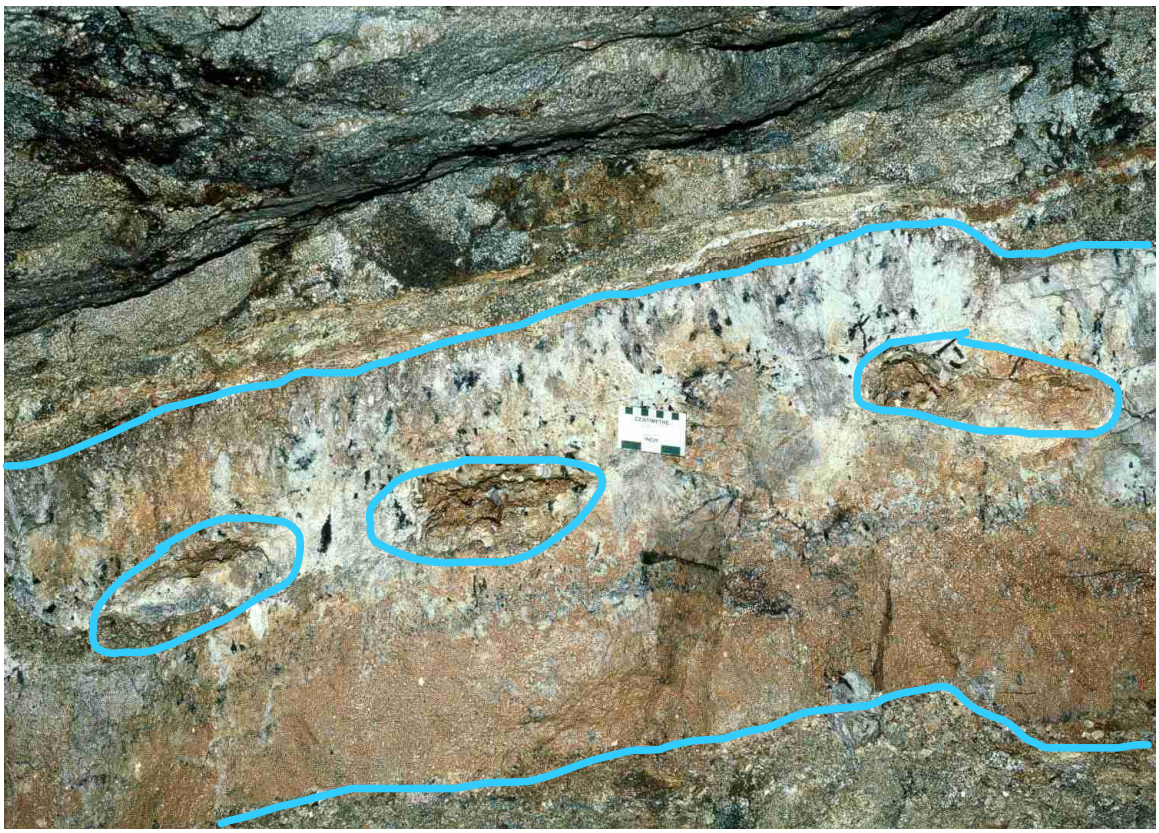

Figure 1. Pegmatite dike from San Diego mine, Mesa Grande, California (Photo from David London). Bottom and top of dike are lined in blue. Circled areas are locations of excavated miarolitic cavities.

Figure 2. Miarolitic cavity from Oceanview mine, Pala, California (Photo from David London). Crystals in center of pocket capped by a white clay on the bottom and a red clay at the top.

Figure 3. Elbaite-filled miarolitic cavity within clay matrix from Himalaya mine, Mesa Grande, California (Photo from Chris Rose)

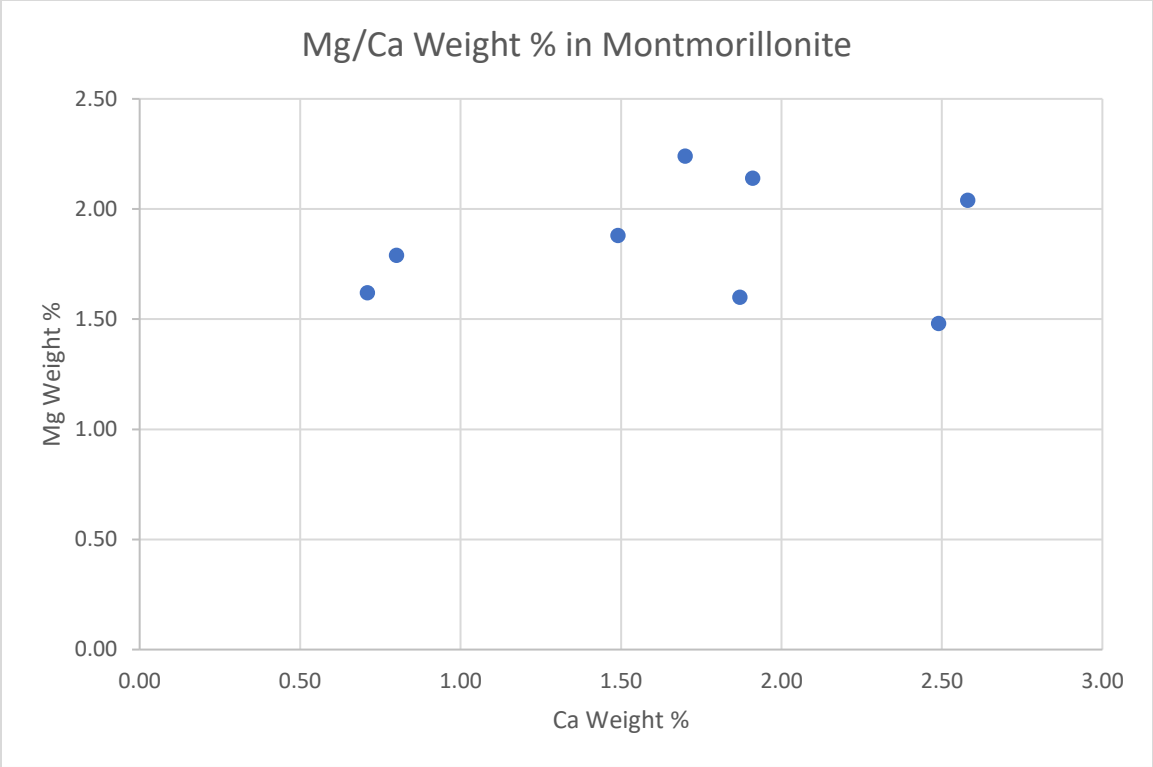

Figure 4. Scatter plot of Mg to Ca weight percent values from EDXA analyses of montmorillonite samples. No correlation of these elements.

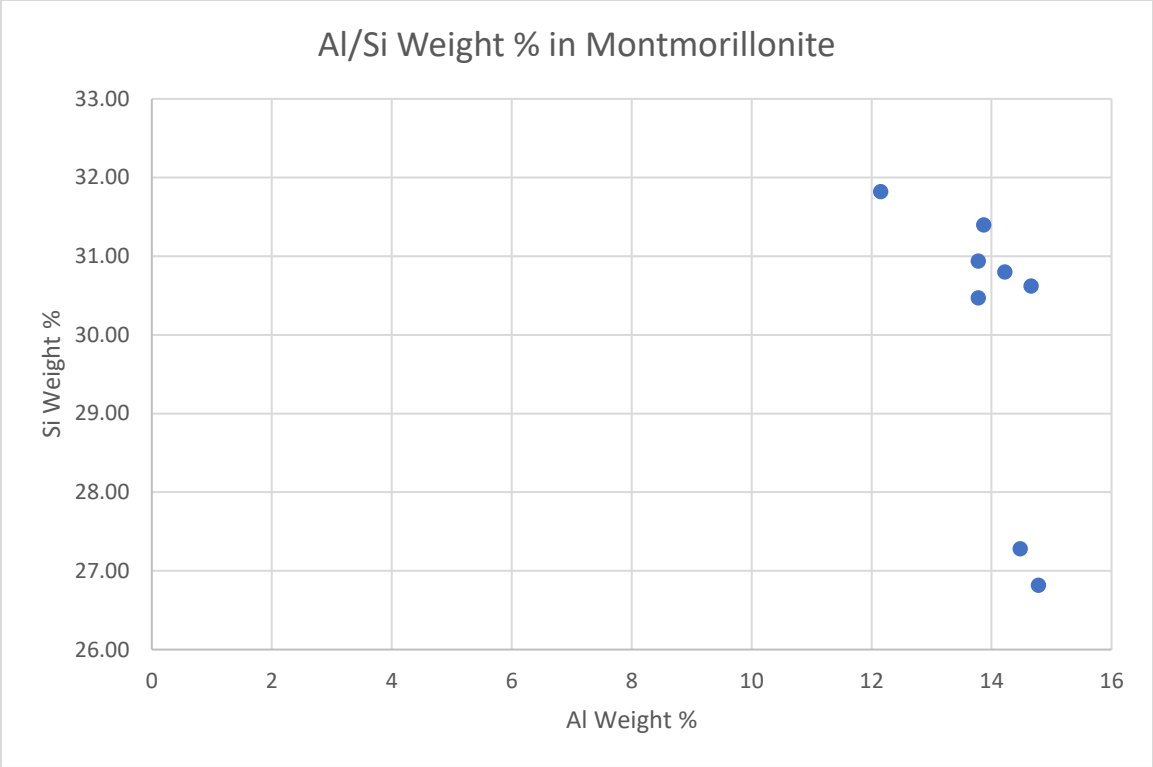

Figure 5. Scatter plot of Al to Si weight percent values from EDXA analyses of montmorillonite samples. No correlation of these elements.

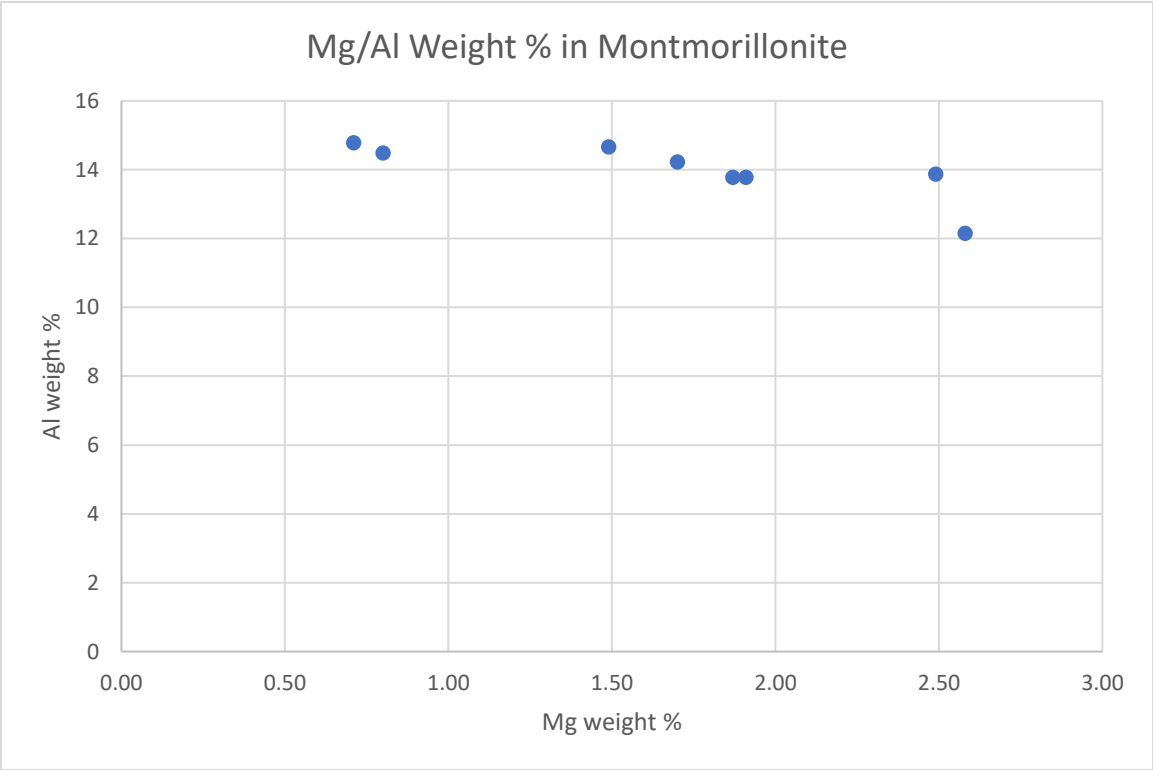

Figure 6. Scatter plot of Al to Mg weight percent values from EDXA analyses of montmorillonite samples. No correlation of these elements.

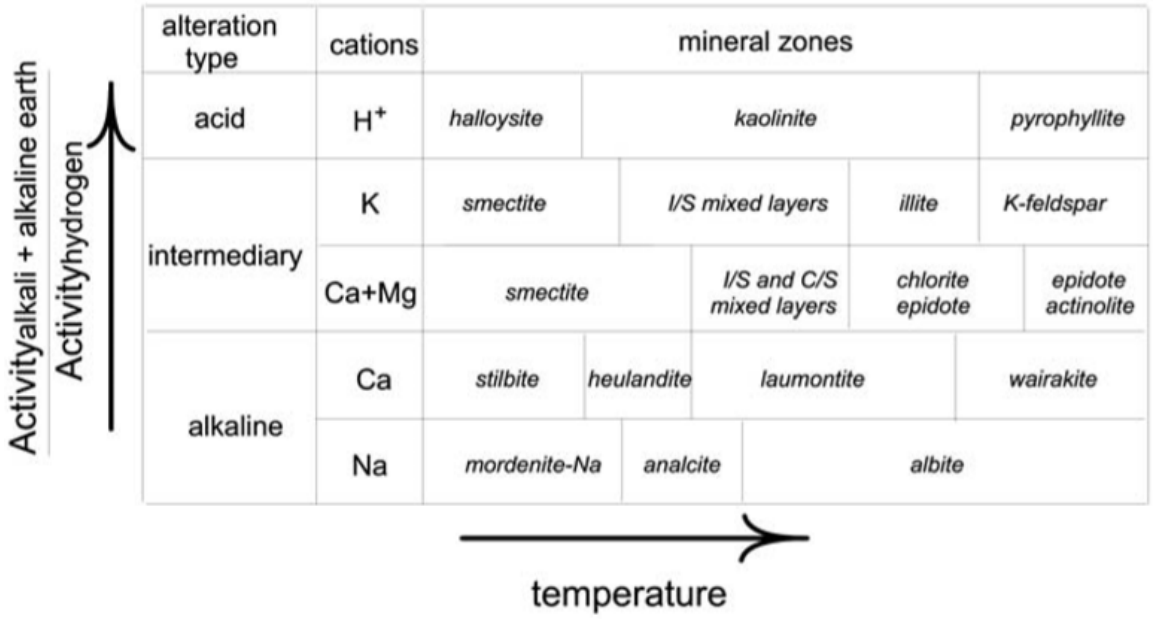

Figure 7. Paragenetic sequence of clay minerals under alkaline to acidic chemical conditions from Meunier (2005). This paragenetic sequence is interpreted to be the same one for the low-temperature minerals in miarolitic cavities.

TABLES

Table 1. Minerals found within miarolitic cavities in pegmatites of Maine and California. Chemical formulas are taken from *Mindat.org*

Group	Mineral	Formula
Smectite	Beidellite	$(Na,Ca_{0.5})_{0.3}Al_2((Si,Al)_4O_{10})(OH)_2 \cdot nH_2O$
	Montmorillonite	$(Na,Ca)_{0.33}(Al,Mg)_2(Si_4O_{10})(OH)_2 \cdot nH_2O$
	Nontronite	$Na_{0.3}Fe_2((Si,Al)_4O_{10})(OH)_2 \cdot nH_2O$
Kaolin	Kaolinite	$Al_2(Si_2O_5)(OH)_4$
	Halloysite	$Al_2(Si_2O_5)(OH)_4$
Oxide	Goethite	$\alpha\text{-}Fe^{3+}O(OH)$
	Todorokite	$(Na,Ca,K,Ba,Sr)_{1-x}(Mn,Mg,Al)_6O_{12} \cdot 3\text{-}4H_2O$
Chlorite	Clinochlore	$Mg_5Al(AlSi_3O_{10})(OH)_8$
	Cookeite	$(Al_2Li)Al_2(AlSi_3O_{10})(OH)_8$
Zeolite	Heulandite	$(Ca,Na)_5(Si_{27}Al_9)O_{72} \cdot 26H_2O$
	Laumontite	$CaAl_2Si_4O_{12} \cdot 4H_2O$
	Stilbite	$NaCa_4[Al_9Si_{27}O_{72}] \cdot nH_2O$
Other Phyllosilicate	Palygorskite	$(Mg,Al)_5(Si,Al)_8O_{20}(OH)_2 \cdot 8H_2O$
	Tosudite	$Na_{0.5}(Al,Mg)_6((Si,Al)_8O_{18})(OH)_{12} \cdot 5H_2O$
Mica	Lepidolite	$K(Li,Al)_3(Al,Si)_4O_{10}(F,OH)_2$
	Muscovite	$KAl_2(AlSi_3O_{10})(OH)_2$
Primary-formed minerals	Alkali feldspar	$KAlSi_3O_8$
	Beryl	$Be_3Al_2(Si_6O_{18})$
	Elbaite tourmaline	$Na(Li_{1.5}Al_{1.5})Al_6(Si_6O_{18})(BO_3)_3(OH)_3(OH)$
	Montebrasite	$LiAl(PO_4)(OH)$
	Plagioclase	$(Na,Ca)Al_{1\text{-}2}Si_{2\text{-}3}O_8$
	Pollucite	$(Cs,Na)_2(Al_2Si_4O_{12}) \cdot 2H_2O$
	Quartz	SiO_2
	Spodumene	$LiAlSi_2O_6$
	Topaz	$Al_2(SiO_4)(F,OH)_2$

Table 2. Summary of all the minerals present within the clay samples analyzed using x-ray diffraction. M is representative of the major mineral, m is representative of the minor minerals, and tr is representative of the trace minerals.

Sample	Color	Texture	Kaolinite	Montmorillonite	Illite	Chlorite	Albite	Quartz	Goethite	Laumontite	Microcline	Halloysite	Todorokite	Cookeite
MM 001	pistachio/tan	cohesive	m	M										
MM 003	salmon	cohesive	m	M	tr									
MM 002	rust	powder	m	tr	M	tr	tr	tr	tr					
HAV 001	white	cohesive	M	tr	tr									
HAV 002	white	cohesive	M	tr										
HIM 025	rust	sticky	M	m	m									
HIM 026	dark pink	cohesive		M										
HIM 027	white	granular			m		m			M	tr			
HIM 028	pale pink	powder	m	M										
OVU 001	rust	sticky	M	m	m									
OVU 002	dark pink	cohesive	m	M										
OVU 003	dark pink	powder	m	M										
OVU 004	pale pink	powder	tr	M									tr	
OVU 005	rust	sticky	M	m	m									
OVU 007	pale pink	powder		M										
PbN Mbr clay	white	cohesive												M

Table 3. Montmorillonite chemical varieties from the ICDD database present within the clay samples

Phase ID	Chemical Formula	PDF-#	Present in Samples
Montmorillonite	$Na_{0.3}(Al,Mg)_2Si_4O_{10}(OH)_2 \cdot xH_2O$	00-058-2010	HIM 026, OVU 003
Montmorillonite	$(Ca,Na)_{0.3}Al_2(Si,Al)_4O_{10}(OH)_2 \cdot xH_2O$	00-058-2039	MM 1, MM 3, HIM 028, OVU 002, OVU 004, OVU 007
Montmorillonite	$Ca_{0.2}(Al,Mg)_2Si_4O_{10}(OH)_2 \cdot 4H_2O$	00-013-0135	OVU 007

Table 4. Elemental signatures of the montmorillonite dominant clay samples using EDXA, normalized to 11 oxygen atoms

	O		Na		Mg		Al		Si		K		Ca	
Sample	Wt. %	# Cat.	Wt. %	# Cat.	Wt. %	# Cat.	Wt. %	# Cat.	Wt. %	# Cat.	Wt. %	# Cat.	Wt. %	# Cat.
MM 1	50.03S	--	0.020	0.003	1.870	0.270	13.78	1.797	30.94	3.875	0.000	0.000	1.600	0.140
MM 3	50.08S	--	0.010	0.002	1.700	0.246	14.22	1.852	30.80	3.854	0.000	0.000	2.240	0.196
OVU 002	47.88S	--	0.020	0.004	0.710	0.107	14.78	2.014	26.82	3.509	0.000	0.000	1.620	0.149
OVU 003	47.86S	--	0.000	0.000	0.800	0.121	14.48	1.973	27.28	3.573	0.030	0.003	1.790	0.164
OVU 004	49.66S	--	0.000	0.000	1.910	0.279	13.78	1.810	30.47	3.845	0.000	0.000	2.140	0.189
OVU 007	49.98S	--	0.000	0.000	2.580	0.373	12.15	1.586	31.82	3.989	0.000	0.000	2.040	0.179
HIM 026	50.07S	--	0.000	0.000	1.490	0.216	14.66	1.910	30.62	3.832	0.000	0.000	1.880	0.165
HIM 028	50.41S	--	0.000	0.000	2.490	0.357	13.87	1.794	31.40	3.903	0.000	0.000	1.480	0.129

	Ti		Mn		Fe		Cs		Ba		Total	
Sample	Wt. %	# Cat.	Wt. %	# Cat.	Wt. %	# Cat.	Wt. %	# Cat.	Wt. %	# Cat.	Wt. %	# Cat.
MM 1	0.050	0.004	0.230	0.015	1.230	0.078	0.240	0.006	0.000	0.000	100.0	6.189
MM 3	0.000	0.000	0.220	0.014	0.570	0.036	0.040	0.001	0.130	0.003	100.0	6.204
OVU 002	0.110	0.008	3.420	0.229	4.630	0.305	0.000	0.000	0.000	0.000	100.0	6.325
OVU 003	0.040	0.003	4.420	0.296	3.050	0.201	0.030	0.001	0.230	0.006	100.0	6.339
OVU 004	0.030	0.002	1.830	0.118	0.000	0.000	0.000	0.000	0.180	0.005	100.0	6.248
OVU 007	0.000	0.000	1.400	0.090	0.000	0.000	0.000	0.000	0.030	0.001	100.0	6.218
HIM 026	0.010	0.001	0.920	0.059	0.300	0.019	0.040	0.001	0.000	0.000	100.0	6.203
HIM 028	0.020	0.001	0.050	0.003	0.080	0.005	0.180	0.005	0.040	0.001	100.0	6.198

Table 5. Al/Si order values (Σt_1) of the alkali feldspar samples calculated from XRD peaks and equations for monoclinic and triclinic feldspars from Krolle and Ribbe (1987).

	Σt_1	
Sample	Monoclinic	Triclinic
HIM 024	0.85	0.85
WQU 3	0.94	0.95
OVU 008	0.89	0.89
LT3 048	0.85	0.86
LT3 044 rim	0.97	0.98
LT3 044 core	0.92	0.93
PbN Mbr PK#1 rim	0.90	0.91
PbN Mbr PK#1 core	1.02	1.01